USGS
science for a changing world

A Method for Determining Avian Influenza Virus Hemagglutinin and Neuraminidase Subtype Association

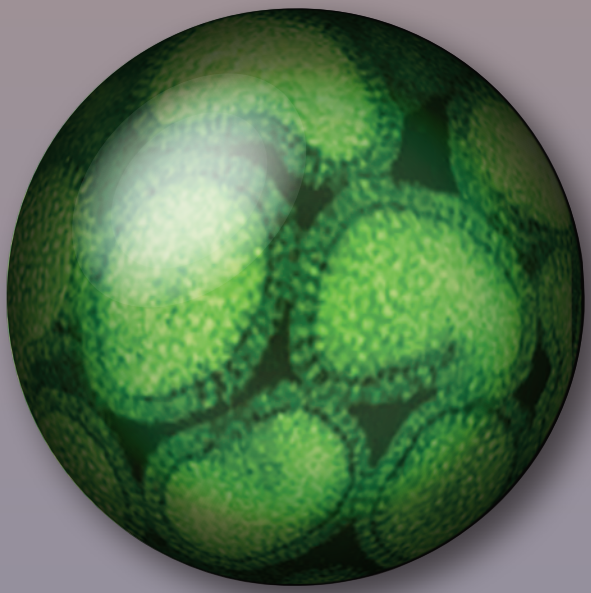

Open-File Report 2018–1102

U.S. Department of the Interior
U.S. Geological Survey

Cover. Photograph of a blue-winged teal by Andy Ramey, U.S. Geological Survey, on March 29, 2013, and image of avian influenza virus modified from photograph by Andy Ramey, U.S. Geological Survey on March 29, 2013.

A Method for Determining Avian Influenza Virus Hemagglutinin and Neuraminidase Subtype Association

By Christopher A. Ottinger, Deborah D. Iwanowicz , Luke R. Iwanowicz, Cynthia R. Adams, Lakyn R. Sanders, and Christine L. Densmore

Open-File Report 2018–1102

U.S. Department of the Interior
U.S. Geological Survey

U.S. Department of the Interior
RYAN K. ZINKE, Secretary

U.S. Geological Survey
James F. Reilly II, Director

U.S. Geological Survey, Reston, Virginia: 2018

For more information on the USGS—the Federal source for science about the Earth, its natural and living resources, natural hazards, and the environment—visit https://www.usgs.gov or call 1–888–ASK–USGS.

For an overview of USGS information products, including maps, imagery, and publications, visit https://store.usgs.gov.

Suggested citation:
Ottinger, C.A., Iwanowicz, D.D., Iwanowicz, L.R., Adams, C.R., Sanders, L.R., and Densmore, C.L.,2018, A method for determining avian influenza virus hemagglutinin and neuraminidase subtype association: U.S. Geological Survey Open-File Report 2018–1102, 15 p., https://doi.org/10.3133/ofr20181102.

ISSN 2331–1258 (online)

Contents

Figures

Tables

Conversion Factors

International System of Units to U.S. customary units

Multiply	By	To obtain
	Volume	
liter (L)	33.814	ounce, fluid (fl. oz)
	Mass	
gram (g)	0.035274	ounce, avoirdupois (oz)

Temperature in degrees Celsius (°C) may be converted to degrees Fahrenheit (°F) as follows:

$$°F = (1.8 \times °C) + 32.$$

Temperature in degrees Fahrenheit (°F) may be converted to degrees Celsius (°C) as follows:

$$°C = (°F - 32) / 1.8.$$

Supplemental Information

Concentrations of chemical constituents are given in nanogram per microliter (ng µL-1) or nanomole per liter (nmol/L)

Abbreviations

AIV	avian influenza virus
BLAST	basic local alignment search tool
BP	base pairs
cDNA	complementary deoxyribonucleic acid
CV	cumulative variance
HA	hemagglutinin
HPAIV	high pathology avian influenza virus
NA	neuraminidase
NCBI	National Center for Biotechnology Information
NF	Nuclease free
qPCR	quantitative polymerase chain reaction
RNA	ribonucleic acid
RT-PCR	reverse transcription polymerase chain reaction
RT-qPCR	reverse transcription quantitative polymerase chain reaction
USGS	U.S. Geological Survey

A Method for Determining Avian Influenza Virus Hemagglutinin and Neuraminidase Subtype Association

By Christopher A. Ottinger, Deborah D. Iwanowicz , Luke R. Iwanowicz, Cynthia R. Adams, Lakyn R. Sanders, and Christine L. Densmore

Abstract

Methods for grouping specific avian influenza virus (AIV) hemagglutinin (HA) and neuraminidase (NA) subtype reverse-transcription polymerase chain reaction (RT-PCR) products into HA:NA subtypes when egg incubation is technically not feasible were evaluated. These approaches were adopted for use as post hoc methods after melt curve analysis. The methods are based on ratios obtained from amplicon copy count and amplicon molarity and were founded on the premise that infectious particles contain an equal copy count of single-stranded ribonucleic acid segments that encode HA or NA, and thus subtype-specific amplicons from a single AIV isolate should yield a theoretical HA:NA ratio of 1. Single and mixed HA:NA AIV subtype samples were evaluated to determine whether the calculated HA:NA ratios would approach the theoretical value. With these samples, preference was given to the molarity methods to better define and correct for the effects of multiple potential amplicons in the amplification mix. Further, the molarity method was used to evaluate pond sediment spiked with intact virus of known HA:NA subtype to determine whether the method is sufficiently robust to be used with complex samples, such as those acquired from waterfowl habitat. This was a proof-of-concept study intended to guide future methods development. The methods here are not meant to be applied in any other context.

From the analysis of fully characterized isolates of North American AIV, the HA:NA molarity-based ratios were found to be 1.63 ± 0.75 (mean ± standard deviation) when corrected for the difference in amplification strength and the production of multiple amplicons in some reactions using equations developed in this study. Copy count HA:NA ratios, obtained from HA and NA subtype (RT-qPCR), were 1.146 ± 0.124 (mean ± standard deviation) when corrected for amplification efficiency. Correct associations of HA:NA subtype sample composition were made with mixed samples containing 1 HA and 2 NA, and 2 HA and 2 NA. When spiked pond sediment was evaluated, the molar ratio obtained for the H4 and N6 identified in the sample was 1.28 with correction and 1.14 without correction.

Background

Avian influenza virus (AIV) poses global threats to food production from domestic animal and human health (Machalaba and others, 2015). Consequently, surveillance programs for AIV in waterfowl populations, and recently (2018) environmental reservoirs, are of increasing importance (Lang and others, 2008). A subset of the known hemagglutinin (HA) subtypes is associated with high pathology AIV (HPAIV). Although changes in HA gene segments are recognized as major components in the transformation of low pathology AIV to HPAIV, changes in neuraminidase (NA) gene segments are also known to contribute to this transformation (Stech and others, 2015). The role of multiple gene segments in the development of HPAIV emphasizes the importance of recognizing not only individual HA and NA subtypes, but also the combined HA:NA subtypes in AIV surveillance programs.

Our interest is in the direct molecular-based characterization of AIV from environmental samples to the level of HA:NA associated subtypes without the need for virus amplification by cell culture. Typical AIV screening utilizes quantitative polymerase chain reaction (qPCR) methodology that includes the use of subtype-specific TaqMan probes for selected virulent subtypes (Payungporn and others, 2006). Holistic screening of AIV diversity in the environment may yield a better understanding of viral ecology. Methods that utilize degenerate primers that amplify the full repertoire of known HA and NA subtypes have been developed (Tsukamoto and others, 2012) but are problematic in terms of HA:NA subtype associations. When single HA and NA subtype genes are characterized from a sample, questions remain as to whether additional subtypes have been lost during the isolation and characterization process. When multiple AIV subtypes are present in a sample, the association of HA and NA into specific HA:NA subtypes can be impossible without additional information. Here we suggest an alternative method for HA:NA subtype association that can assist in this process.

TaqMan- and SYBR Green-chemistry methods have been used in combination with reverse transcription quantitative polymerase chain reaction (RT-qPCR) to evaluate samples for the presence of AIV. The former method is effective for

diagnostic screening when the exact target AIV subtype is known because the inclusion of a probe increases assay specificity (Payungporn and others, 2006). The latter method has proven useful for surveillance when used with degenerate primer sets that target all known HA and NA subtype genes, where copy count and melt curve analyses are used to determine specificity (Tsukamoto and others, 2012). Tsukamoto and others (2012) produced sample-specific HA and NA subtype lists. This product type, produced from PCR-based AIV genome copy detection, is like that obtained using antibody-based AIV protein detection (Bowman and others, 2015). Product type is the only similarity between these two methods, making direct comparisons of HA and NA subtypes ambiguous. Neither method yields HA:NA subtype associations.

When using TaqMan-chemistry, the grouping of HA and NA subtypes into an HA:NA subtype association occurs by default because only one HA subtype and one NA subtype are targeted using highly specific probes and type-specific methods validation (Payungporn and others, 2006). Alternatively, nothing may be detected, or a single subtype may be detected resulting in a failed or incomplete analysis. A benefit of probe specificity with TaqMan-chemistry is that it increases outcome confidence but it also limits detection when subtype sequence variation or subtype re-assortment occurs. This limitation makes the method less than ideal for environmental surveillance projects intended to detect sequence variation or subtype re-assortment.

When using intercalating dye chemistries such as SYBR Green and primer sets for multiple HA and NA subtypes, which are degenerate to accommodate type-specific sequence variation (Tsukamoto and others, 2012), the confidence associated with high probe specificity is exchanged for breadth of the subtype-specific isolate amplification. Unlike the results obtained using TaqMan-chemistry, when SYBR Green-chemistry is used with multiple subtype primers, no means for subtype association into HA:NA grouping is afforded. Detection of multiple HA and (or) NA subtypes in a single sample can make the determination of HA:NA subtypes problematic without additional information. In theory, the subtype copy count could be used to associate subtypes into HA:NA subtypes because the Influenza A genome consists of single copies of the HA and NA genes (Cheung and Poon, 2007). The copy count ratio of two subtypes that associate to form an HA:NA grouping should approach 1.00. The difficulty with this approach is that validation over a broad range of potential sample mixtures is required. Here, we suggest an alternative solution for the association of HA and NA subtypes into specific HA:NA subtypes and compare the results to results obtained from copy count determinations.

Our alternative approach is a modification of RT-qPCR melt curve analysis (Tsukamoto and others, 2012) using SYBR Green-chemistry and multiple HA and NA primer sets. Applying the same reasoning as used in copy count ratios, we propose the use of molar ratios. Molar ratios are broadly used to describe the composition of complex biomolecules and cellular structures, characterize biochemical interactions, and differentiate normal versus disease states at the subcellular and molecular levels. We are simply applying a classic and well described concept in a different way.

In this proof-of-concept study we evaluated the potential for the practical use of subtype-specific amplicon copy count and molarity in AIV HA:NA subtype association when high throughput sequencing methods are not possible. This approach is applicable to environmental samples containing single or multiple AIV HA:NA groupings. As such, multiple single HA:NA subtypes representing common North American subtypes as well as mixtures of these HA:NA subtypes were evaluated starting with ribonucleic acid (RNA) from fully characterized AIV isolates. As a proof-of-concept, the intent of this study is to inform the development of future methods, and thus the methods here are not meant to be applied in any other context.

This report discusses the methods used in the new alternative approach. Results of this approach are presented in tables and figures.

Methods

RNA extracted from characterized isolates of multiple subtypes was provided by U.S. Geological Survey (USGS) Alaska Science Center, Anchorage, Alaska (table 1) (Pearce and others, 2009; Pearce and others, 2010; Ramey and others; 2010a; Ramey and others, 2010b; Pearce and others, 2011; Ramey and others, 2011; Reeves and others, 2013). Viral RNA was reverse transcribed using the Applied Biosystems high-capacity complementary deoxyribonucleic acid (cDNA) reverse transcription kit (Life Technologies, Carlsbad, California) with random hexamers from the manufacturer's protocol.

All HA and NA subtypes were analyzed on an Applied Biosystems ViiA 7 real-time qPCR (Life Technologies, Carlsbad, Calif.). PCR with a melt curve analysis was performed as described by Tsukamoto and others (2012) but with modifications. The 20-microliter (μL) reaction mixture contained Applied Biosystems Power SYBR Green PCR Master Mix (Life Technologies, Carlsbad, Calif.), 2 micromoles (μM) of forward and reverse primers (table 2), and 1 μL of cDNA. The cDNA was not normalized prior to amplification nor were starting concentrations measured. The melt curve was used to confirm successful amplification of the correct amplicon using dissociation temperature as described in Tsukamoto and others (2012). Each reaction was run in duplicate except for the control reactions, which were run in triplicate. Replicates were pooled prior to purification.

Post-amplification product purification was performed using the QIAquick PCR Purification Kit and following the manufacture's protocol (Qiagen, Valencia, Calif.). All purified RT-qPCR) products were evaluated using an Agilent Bioanalyzer with Expert Software (Agilent Technologies, Santa Clara, Calif.) with Agilent DNA 1000 Kits and following the manufacturer's protocols. Analysis was performed

using the default setting, except for height threshold which was reduced to 5 fluorescent units. Potential target amplicons were identified based on maximum observed amplicon molarity determined from subtype-specific reaction products that fell within the assay sensitivity range of 0.1–50 nanograms per microliter (ng µL-1) (Agilent Technologies) and within the size range of 100–400 base pairs (bp; Tsukamoto and others, 2012). Amplicons from all reactions were sequenced in both directions using Applied Biosystems Big Dye Cycle Sequencing Kit (Foster City, Calif.) to confirm nucleotide sequence. The sequencing reaction profile used consisted of 30 cycles of 20 seconds at 96 degrees Celsius (ºC), 20 seconds at 58 ºC, and 4 minutes at 60 ºC, with a 10-minute extension at 72 °C. The sequencing reactions were cleaned with Agencourt CleanSEQ (Beckman Coulter Genomics, Beckman Coulter Inc., Brea, Calif.), following manufacturer's instructions. Sequencing was carried out on an Applied Biosystems 3130xl Genetic Analyzer (Foster City, Calif.). Biomatters Limited, Geneious R6 software (San Francisco, Calif.) was used to trim and align sequences. Finalized sequences were compared with those published for the specific isolates from which the target amplicons were

Table 1. Isolates of avian influenza viruses from paired cloacal and oropharyngeal swabs inoculated into specific-pathogen-free eggs post screening, purified, and characterized.

[HA, hemagglutinin; NA, neuraminidase; NCBI, National Center for Biotechnology Information; H, identifies hemagglutinin gene; N, identifies neuraminidase gene]

Isolate	HA	NA	NCBI accession number HA	NCBI accession number NA	Literature cited
3455	H1	N9	HM059985	HM060041	Ramey and others, 2010b
48944	H1	N1	GU168283	GU168373	Ramey and others,2010a
48982	H1	N1	GU168288	GU168374	Ramey and others, 2010a
49176	H1	N1	GU168289	GU168367	Ramey and others, 2010a
100756	H1	N1	GQ411892	GQ411894	Pearce and others, 2010
103775	H1	N1	HM193551	HM193628	Pearce and others, 2011
44927	H10	N7	GU168309	GU168402	Ramey and others,2010a
44939	H10	N7	GU168308	GU168401	Ramey and others, 2010a
79190	H10	N9	HM059988	HM060036	Ramey and others, 2010b
100870	H10	N1	JF323753	JF323778	Ramey and others,2011
134560	H10	N7	JX080780	JX081172	Reeves and others, 2013
40459	H11	N9	JX080738	JX081129	Reeves and others,2013
101124	H11	N9	JF323755	JF323789	Ramey and others, 2011
103717	H11	N9	HM193587	HM193665	Pearce and others, 2011
2355	H2	N1	JX080736	JX081127	Reeves and others, 2013
2366	H2	N1	JX080744	JX081135	Reeves and others, 2013
2390	H2	N5	JX080748	JX081139	Reeves and others, 2013
32425	H2	N2	JX080751	JX081142	Reeves and others, 2013
32921	H2	N3	JX080765	JX081157	Reeves and others, 2013
13526	H3	N8	HM193560	HM193661	Pearce and others, 2011
16080	H3	N8	HM193556	HM193660	Pearce and others, 2011
37536	H3	N8	JX080757	JX081148	Reeves and others, 2013
44303	H3	N8	GU143843	GU168410	Ramey and others, 2010a
45315	H3	N6	GU143852	GU168393	Ramey and others, 2010a
45321	H3	N8	GU143850	GU168416	Ramey and others, 2010a
104839	H3	N6	HM193566	HM193651	Pearce and others, 2011
254	H4	N7	JX080760	JX081151	Reeves and others, 2013
15913	H4	N6	HM193578	HM193653	Pearce and others, 2011
38800	H4	N6	JX080742	JX081133	Reeves and others, 2013
49090	H4	N6	GU168299	GU168395	Ramey and others, 2010a
60390	H4	N6	HM193576	HM193652	Pearce and others, 2011
103889	H4	N6	HM193574	HM193650	Pearce and others, 2011
884	H5	N2	JX080782	JX081174	Reeves and others, 2013
926	H5	N2	JX080783	JX081175	Reeves and others, 2013
945	H5	N2	JX080784	JX081176	Reeves and others, 2013
2216	H5	N2	JX080785	JX081177	Reeves and others, 2013
3850	H5	N2	JX080756	JX081147	Reeves and others, 2013
13618	H6	N2	FJ520080	FJ520139	Pearce and others, 2009
52796	H6	N2	GU168302	GU168376	Ramey and others, 2010a
56526	H6	N1	FJ520106	FJ520164	Pearce and others, 2009
2320	H7	N7	JX080762	JX081154	Reeves and others, 2013

obtained using the National Center for Biotechnology Information (NCBI) nucleotide Basic Local Alignment Search Tool (BLAST). The size (bp) of confirmed target amplicons was used to generate average amplicon sizes for each HA and NA subtype evaluated in this study.

The copy counts for HA and NA genes in each isolate were quantified using quantitative RT-qPCR. Briefly, RT-qPCR was run using SYBR Green-chemistry with a standard curve for each subtype to calculate the copy count. The RT-qPCR reaction mixture and amplification conditions were the same as those used in melt curve analysis described above. Standards were created using eight dilutions of the purified amplicons from samples of each subtype (table 1) with calculated standard concentrations of 108–101 copies/µL. The relation between HA and NA copy counts from each isolate was evaluated by calculating HA:NA ratios.

Corrected molar ratios were determined using the following equations:

$$\frac{\left(\left(H1SAM\times\left(\frac{H1AS}{N1AS}\right)\right)\times\left(\frac{N1TM}{H1TM}\right)\right)}{N1SAM} \tag{1}$$

$$\frac{ABS\left(\left(H1SAM\times\left(\frac{H1AS}{N1AS}\right)\right)\times\left(\frac{N1TM}{H1TM}\right)\right)-\left(N2SAM\times\left(\frac{H1AS}{N2AS}\right)\times\left(\frac{N2TM}{H1TM}\right)\right)}{N1SAM} \tag{2}$$

and

$$\frac{\left(\left(H1SAM\times\left(\frac{H1AS}{N1AS}\right)\right)\times\left(\frac{N1TM}{H1TM}\right)\right)}{ABS\left(N1SAM-\left(H2SAM\times\left(\frac{H2AS}{N1AS}\right)\times\left(\frac{N1TM}{H2TM}\right)\right)\right)} \tag{3}$$

where

ABS	is	absolute value, in nanomoles;
*H*1*SAM* or *N*1*SAM*	is	specific amplicon molarity of hemagglutinin or neuraminidase subtype under consideration;
*H*1*AS* or *N*1*AS*	is	amplification strength as measured by total fluorescence at the end of the terminal qPCR cycle of hemagglutinin or neuraminidase subtype under consideration;
*H*1*TM* or *N*1*TM*	is	total molarity observed for all amplicons, including the subtype-specific amplicon from subtype-specific product analysis of hemagglutinin or neuraminidase subtype under consideration;
*H*2*SAM* or *N*2*SAM*	is	similar to H1SAM or N1SAM, except that values are those used to correct for the molarity contribution of subtype not considered in ratio;
*H*2*AS* or *N*2*AS*	is	similar to H1AS or N1AS, except that values are those used to correct for the molarity contribution of subtype not considered in ratio; and
*H*2*TM* or *N*2*TM*	is	similar to H1TM or N1TM, except that values are those used to correct for the molarity contribution of subtype not considered in ratio.

Table 2. Primers used for subtyping hemagglutinin and neuraminidase genes of purified and characterized isolates of avian influenza virus reverse transcribed into cDNA from purified RNA and amplified using a real-time reverse transcription polymerase chain reaction.[1]

[cDNA, complementary deoxyribonucleic acid; RNA, ribonucleic acid; bp, base pairs; H, identifies hemagglutinin gene; N, identifies neuraminidase gene; C, cytosine; G, guanine; A, adenine; T, thymine; B, mixed base C/G/T; D, mixed base A/G/T; H, mixed base A/T/C; K, mixed base G/T; M, mixed base A/C; R, mixed base A/G; V, mixed base A/C/G; W, mixed base A/T; Y, mixed base C/T]

Subtype	Size (bp)	Forward sequence	Reverse sequence
H1	305	GATRCWCCAGTYCAYAAYT	TCTGYGTGCTYTTYTGRT
H2	343	AAMMCTTGAAAAYTGYGA	TTCAATYACRGASTTYACYTTG
H3	376	GYATYACTCCWAATGGAAGC	ATYCTYCCTTCYACTTCDGM
H4	284	AGYAARTGYCAYACHGACA	AGYAARTGYCAYACHGACA
H5	261	CCARTRGGKGCKATAAAYTC	GTCTGCAGCRTAYCCACTYC
H6	387	TCARAYYTDCCAATHGAGAA	TCARAYYTDCCAATHGAGAA
H10	311	TCARAYYTDCCAATHGAGAA	TCAGATTCTATGGATTCGAAC
N1	245	TCARTCTGYATGRYAAYTGG	GGRCARAGAGAKGAATTGCC
N2	278	TYTCTMTAACYATTGCRWCARTA	GARTTGTCYTTRGARAAVGG
N6	264	AGGAATGACACTATCSGTAGTAAG	GAYAGRATRTGCCATGAGTTYAC
N7	261	TCWGGAGTGGCMATAGCACT	CACKACCCAYCCTTCAACWTTG
N8	137	CAYATAGYTAGYATYACARTAAC	ACAYTRGYATTGTRCCATTG
N9	227	GTRATAGGCAYRATTGCAGT	CCTYTRGTCARRTTRTTGAA

[1]Post-amplification product purification was performed using the QIAquick PCR.

The equations for corrected molar ratios were derived as modifications of the simple HA:NA ratio. Amplification strength was used to correct for the production of non-target amplicons, a phenomenon associated with SYBR Green-chemistry (Wittwer and others, 1997) that may have a negative effect on final target amplicon concentrations. The use of total molarity had a similar function correct for the occurrence of non-target amplicons in a size range of 100–1,000 bp. Equations used to calculate corrected molarity when two HA:NA subtypes with a shared HA or NA subtype occurred (eqs. 2 and 3) were developed to account for the molarity of one subtype being divided between two other subtypes. The equation for situations where 1 NA and 2 HA subtypes are detected (eq. 3) is provided, but an example is not presented to avoid redundancy.

Target amplicon molarity was taken from the standard Agilent 2100 Expert software output. Total sample molarity was calculated by obtaining the sum of molarities from each double-stranded DNA sample component that was 100–1,000 bp in size and within the quantitative range of the assay. Amplification strength was determined from qPCR output for each reaction by measuring total fluorescence at the end of cycle 30. Standardized values of amplification strength were determined by dividing 1,000,000 by the reaction-specific fluorescence. In this calculation, amplification strength decreases as the standardized values increase. To facilitate ease of comparison, corrected molar ratios calculated to be between 0.01 and 0.99 were converted to a value greater than 1 by dividing 1 by the calculated value.

Chicken-egg allantoic fluid containing viable H4:N6 virus was used to produce a “spiked” pond sediment. Total

RNA was then extracted using a RNA PowerSoil Total RNA Isolation Kit (Mo Bio) and following the manufacture's protocol. Initial virus concentrations were in an expected range of 105–107 virus per milliliter (mL-1) of allantoic fluid (Hon S. Ip, USGS, written commun., 2016). Sediment was obtained from a pond used by overwintering waterfowl and was a mix of silt, sand, and vegetation. Two spiked sediment samples and one negative control sediment sample were evaluated. Each sample and the negative control contained 2.00 ± 0.05 grams (g) of sediment. Total spike volume was 1 mL. The final concentration of the first spike sample was in the range of 105–107 virus per g-1 of sediment. The second spiked sample contained a 1:10 dilution of the first spike with the dilution performed in RNAase- and DNAase-free molecular grade water (NF water). The negative control sample was treated with 1 mL of NF water only. Both alcohol precipitation steps used in the RNA extraction process were performed for 30 minutes at −20 °C. Conversion of extracted RNA to cDNA, RT-qPCR amplification, and analysis of PCR products using the Bioanalyzer were performed as described above.

Table 3. Sanger subtype-specific sequence data obtained for avian influenza virus hemagglutinin and neuraminidase subtype target amplicons from this study.[1]

[H, identifies hemagglutinin gene; N, identifies neuraminidase gene; C, cytosine; G, guanine; A, adenine; T, thymine]

Subtype[1]	Isolate identification[1]	Sequence
H1	3455	GCAACACAAAGTGCCAAACCCCTCACGGGGCCTTGAACAGTAGCCTCCTTTTCAGAATGTGCATCCCATCAC TATTGGAGAATGTCCCAAATATGTCAAGAGCACCAAACTAAGAATGGCAACAGGACTAAGAAATGTACCATC CATTCAATCCAGAGGACTATTTGGAGCAATTGCTGGATTCATTGAAGGAGGATGGACAGGTATGATAGATGGATG GTATGGGTACCACCACCAGAATGAGCAAGGATCAGGATATGCCGCTGACCA
H2	2390	TTGAAAATTGCGAAACTAAATGCCAAACTCCCTTGGGAGCAATAAATACAACATTGCCCTTTCATAATATC CACCCATTGACCATTGGTGAGTGCCCCAAATATGTAAAATCGGAGAGATTGGTCTTGGCAACAGGATTAAGAAAC GTCCCTCAGATTGAATCAAGAGGATTGTTTGGGGCAATAGCTGGTTTCATAGAAGGGGGATGGCAAGGAATGGTT GATGGTTGGTATGGATATCATCACAGCAATGATCAAGGATCCGGGTATGCAGCAGACAAAGAGTCCACT CAGAAGGCAATTGATGGAATCACC
H3	13526	GCATCCCCAATGACAAGCCCTTTCAGAATGTGAACAAGATCACCTACGGAGCATGTCCTAAGTATGTCAAA CAGAGCACTCTGAAACTGGCAACAGGAATGAGGAACGTACCTGAGAAACAAACCAGGGGTCTGTTCGGTG CAATAGCAGGATTTATAGAAAATGGGTGGGAAGGAATGATAGACGGCTGGTATGGTTTCAGACATCAGAACTCT GAGGGTACAGGACAAGCTGCAGACCTAAAAAGCACACAGGCAGCCATCGACCAGATCAATGGGAAATTGAACC GAGTAATCGAGAAAACAAATGAGAAGTTTCATCAGATTGAAAAGGAATT
H4	15913	GACAGGGGTTCAATCACTACCACTAAACCCTTTCAGAACATCTCAAGAATATCAATCGGGGACTGTCCCAAATAT GTCAAACAGGGGTCTTTGAAACTGGCTACAGGGATGAGGAACATCCCTGAGAAGGCAACCAGAGGTCTGTTTG GTGCAATTGCTGGCTTTATAGAGAATGGCTGGCAAGGTTTAATTGATGGGTGGTATGGGTTTAGGCACCAGAATG CAGAAGGGACAGGGACGGCTGCAGATCTC
H4	Intact viron sediment spike	ACCGACAGGGGTTCAATCACTACCACTAAACCCTTTCAGAACATCTCAAGAATATCAATCGGGGACT GTCCCAAATATGTCAAACAGGGGTCTTTGAGACTGGCTACAGGGATGAGGAACATTCCTGAGAAGGCAAC CAGAGGTCTGTTTGGTGCGATTGCTGGCTTTATAGAGAATGGCTGGCAAGGTTTAATTGATGGGTGGTATGGGTT TAGGCACCAGAATGCAGAAGGGACAGGAACGGCTGCAGATCTCAAATCCACTCAGGCAGC
H5	926	ATTGGGGAGTGCCCCAAGTATGTCNAATCGGACAAACTGGTCCTTGCAACAGGACTAAGAAACG TACCCCAAAGAGAAACAAGAGGCCTATTTGGAGCAATAGCAGGATTCATAGAAGGAGGATGGCAAGGAATGGTT GATGGATGGTACGGATACCATCATAGCAATGAGCA
H6	52796	CCAATCGAGAACTGTGATGCCACATGCCAGACTATTGCAGGAGTCCTAAGGACTAATAAAACATTTCAGAATGT GAGTCCTCTGTGGATAGGAGAATGCCCCAAATATGTGAAAAGTGAAAGTTTGAGGCTTGCAACTGGACTGAGA AATGTTCCACAGATTGAGACTAGAGGACTTTTTGGAGCTATCGCAGGATTTATTGAAGGGGGATGGACTGGAAT GATAGATGGGTGGTACGGCTATCACCATGAAAATTCTCAAGGCTCAGGATATGCAGCAGACAAAGAAAGCACT CAAAAGGCTATAGACGGAATTACAAATAAAGTCAATTCCATCATTGACAAAATGAACACACAATTCGAAGCT GTNCNACCACGAA
H10	134560	AATCTTTCCCCGAGAACTGTGGGTCAATGCCCCAAGTATGTGAACAAAAAGAGCCTGTTGCTTGCTACTG GAATGAGGAATGTGCCAGAGGTTGTCCAAGGAAGAGGCCTGTTTGGAGCAATAGCTGGATTCATAGAGAATG GATGGGAAGGAATGGTAGATGGTTGGTATGGTTTCCGACACCAAAATGCCCAAGGCACTGGCCAGGCCGCG GATTATAAAAGTACTCAGGCAGCTATAGATCAAATAACCGGGAAATTGAACAGACTGATAGAGAAGACAAACA CAGAGTTCGAATCCATAGAATCTGAA
N1	48982	TGGAATAATAAGTCTGGTGCTACAAANTGGAAATATAATTTCAATATGGGTTAGCCATTCAATCCAAACTGGAAGT CAGAACTATCCCGAAACATGCAATCAAAGTGTCATTACCTACGAAAACAATACTTGGGTGAATCAGACATACAT CAACATAAGTAATACCAATTTAATTTCAGAACAGGCTGTAGCTCCAGTAACACTAGCAGGCAATTCCTCTCTCT
N2	52796	CANTATGTTTCCTCATGCAAATTGCCATCCTAGCAACGACTATAACACTGCACTTCAAGCAGAATGAATGCAT CATCCCCTCGAACAATCAAGTAGTGCCATGTGAGCCAATCATAGTAGAAAGGAACATAACAGAGATAGTGTATT TAAATAATACCACCATAGAAAGAGAACTTTGTCCTAANTTAACAGANATACAGGGATTGGTCGAAACCACAGTGT CAGATC

Table 3. Sanger subtype-specific sequence data obtained for avian influenza virus hemagglutinin and neuraminidase subtype target amplicons from this study.[1]—Continued

[H, identifies hemagglutinin gene; N, identifies neuraminidase gene; C, cytosine; G, guanine; A, adenine; T, thymine]

Subtype[1]	Isolate identification[1]	Sequence
N6	60390	GGGGCTGAACATTGGGCTTCATTTCAAGGTAGGAGACACACCAGAACCAGGACCCCCTAGTACCAATGAGA CAAACTCCACAACCGCAATAATCAATTACAACACCCAAAACAACTTCACAAATGTGACCAACATTGTGTTGATTA AAGAAGAAAACAAAATGTTCACNANCCTTTCTAAGCCCTTGTGTGAAGTN
N6	Intact viron sediment spike	GCTGAACATTGGGCTTCATTTCAAGGTAGGAGACACACCAGAAACAGGAACCCCTAGTACCAATGAGA CAAACTCCACAACCACAATAATCAACTACAACACCCAAAACAACTTCACAAATGTGACCAACATTGTGTTAATTA AAAAAGAAAACAAAATGTTCACAAACCTTTCTAAGCCCTTGTGTGAAGTGAACTCATGGCACATCCT
N7	134560	TGGCCATAGCACTGAGTATCCTCAACCTACTAATAGGAATATCCAATGTGGGACTGAATGTCTCACTACACCTA AAGGGAAGCAGTAATCAGGATAGAAATTGGACATGCACGAGTGTAACACAAAACAATACGACTTTAATTGAAAA CACATATGTCAACAATACTACTGTCATCAATAAGGAAACAGGGACTGCAAAGCCAAATTATCTAATGCTGAA CAAGAGCTTATGC
N8	13526	ATAGTTAGCATTACAGTAACAGTGTTAGTTCTCCCTGGAAATGGAAATAATGGGGGTTGCAATGAANCAGT CATTAGGGAATACAATGAAACAGTAAGAGG-TTGAGAAGG-TAACACAATTTACCAATGTC
N9	10124	GCAGTACTCATAGGAATAGCAAACCTAGGGTTGAACATAGGGCTACATCTGAAACCAAACTGCAACTGCT CACACTCACAACCTGAAGCAACCAATGCAAGCCAAACAATAATAAACAACTACTATAACGAAACAAACAT CACCCAAATAAGCAATACCAACATCCAAATGGAGGAGAAAGCAAATAGAGAATT

[1]Isolates used in this study. For additional information see table 1.

Table 4. Representative nucleotide BLAST data for Sanger sequences obtained for avian influenza virus hemagglutinin and neuraminidase subtype target amplicons from this study.

[BLAST, Basic Local Alignment Search Tool; H, identifies hemagglutinin gene; N, identifies neuraminidase gene; NCBI, National Center for Biotechnology Information]

Subtype[1]	Isolate identification[1]	NCBI accession number for published data[1]	BLAST metrics					
			Sequence range	Score	Query cover	Expected (E value)	Identities	Gaps
H1	3455	HM059985	885–1,152 (268)	496	98%	2E−144	100%	0%
H2	2390	JX080748	871–1,182 (312)	577	99%	9E−169	100%	0%
H3	13526	HM193560	913–1,249 (337)	623	100%	0.0	100%	0%
H4	15913	HM193578	888–1,139 (252)	466	100%	2E−135	100%	0%
H4	Intact virus sediment spike	CY076205.1	896–1,167 (272)	492	99%	2E−135	99%	0%
H5	926	JX080783	914–1,086 (173)	316	100%	1E−90	99%	0%
H6	52796	GU168302	835–1,212 (378)	673	100%	0.0	99%	0%
H10	134560	JX080780	908–1,224 (317)	575	99%	1E−166	99%	0%
N1	48982	GU168374	18–259 (230)	425	99%	6E−123	98%	0%
N2	52796	GU168376	29–252 (219)	405	98%	2E−117	99%	0%
N6	60390	HM193652	84–278 (191)	353	99%	8E−102	99%	0%
N6	Intact virus sediment spike	CY076191.1	96–302 (207)	377	98%	5E−11	99%	0%
N7	134560	JX081172	20–252 (233)	431	100%	4E−125	100%	0%
N8	13526	HM193661	72–206 (135)	241	100%	4E−68	99%	0%
N9	10124	JF323789	75–268 (194)	359	100%	2E−103	100%	0%

[1]Isolates used in this study. For additional information see table 1.

Results and Discussion

Development of these assays was intended to be applied as a post hoc analysis of the Tsukamoto and others (2012) melt curve method. The use of RT-qPCR and molar ratios as described here is strictly intended as a component in the characterization of environmental samples that are evaluated using molecular methods only. Fragment size analysis provides confirmation of amplicon size and an opportunity to determine molar ratios in the presence of multiple HA:NA subtypes in a single sample. AIV genomic RNA from egg culture was used to validate the suggested method.

Subtype-specific sequence data (table 3) for potential target amplicons were consistent with the published data for the isolates from which the amplicons were produced (table 4).

Isolate specific copy count HA:NA ratios obtained from HA and NA subtype RT-qPCR were 1.146 ± 0.124 (mean ± standard deviation). Ratio values ranged from 1.028 to 1.509. Statistical metrics for the RT-qPCR, including amplification efficiency (table 5) and isolate specific subtype copy counts (table 6), are provided. Electropherograms for HA (fig. 1) and NA (fig. 2), including amplicon size and molarity values, are typical of Bioanalyzer DNA 1000 chip output when evaluated using Agilent 2100 Expert software to compare amplicons with the included standard ladder. Based on the ladder as the sample, the Agilent DNA 1000 performance metrics are as follows (Agilent Technologies): sizing accuracy of ± 10 percent, a sizing reproducibility of 5-percent cumulative variance (CV), quantitation accuracy of 20 percent CV, and quantitation reproducibility

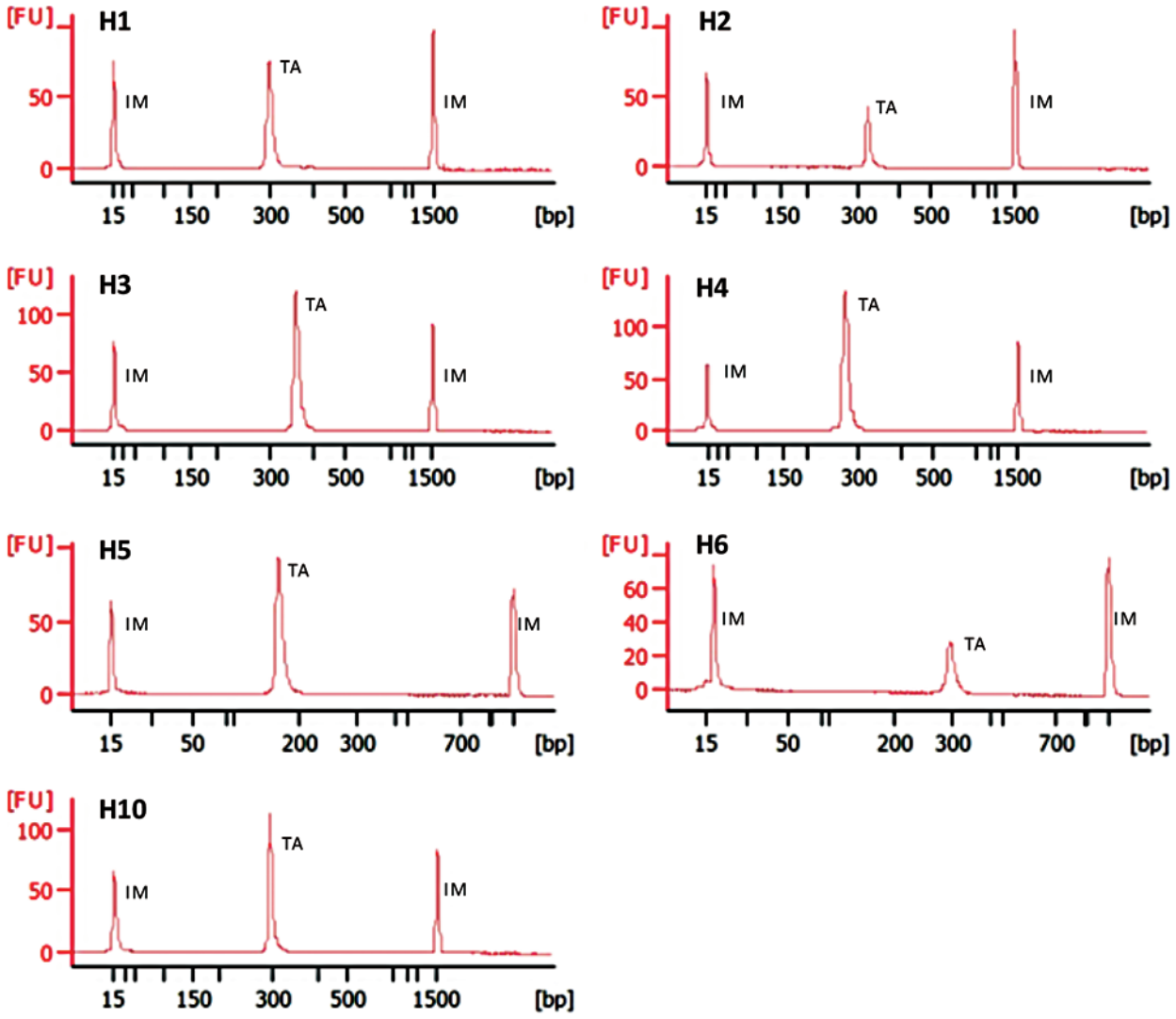

Figure 1. Typical electropherograms hemagglutinin subtypes evaluated in this study as produced by Agilent's Bioanalyzer DNA 1000 and Agilent's 2100 Expert software. Analyses produced from purified and characterized isolates reverse transcribed into deoxyribonucleic acid from purified ribonucleic acid, amplified by reverse transcription quantitative polymerase chain reaction, and then evaluated for amplicon size and molarity. Subtype identification is associated with each graph.

(bp, base pair; FU, fluorescent unit; H, identifies hemagglutinin gene; IM, internal marker; TA, subtype-specific target amplicon)

Table 5. Quantitative real-time reverse transcription polymerase chain reaction linear regression statistics for hemagglutinin and neuraminidase gene standards used in the assessment of gene copy counts present in the ribonucleic acid from avian influenza virus used in this study.

[r^2, coefficient of determination; H, identifies hemagglutinin gene; N, identifies neuraminidase gene]

Subtype	Slope	y-intercept	r^2	Percent amplification efficiency	Error
H1	−3.818	41.829	1	82.778	0.016
H2	−3.442	35.125	0.996	95.968	0.043
H3	−3.831	38.908	0.996	82.402	0.055
H4	−3.644	40.997	0.997	88.102	0.054
H5	−3.648	39.442	0.992	87.998	0.068
H6	−3.711	37.791	0.997	85.972	0.045
H10	−3.427	37.992	0.998	95.798	0.034
N1	−3.37	38.073	0.984	98.036	0.121
N2	−4.326	45.098	0.992	70.27	0.09
N6	−3.334	36.952	0.992	99.499	0.062
N7	−0.354	36.199	0.997	92.91	0.045
N8	−3.872	41.275	0.999	81.255	0.019
N9	−3.822	39.307	0.998	82.645	0.036

Table 6. Copy count of hemagglutinin and neuraminidase genes obtained from gene copy counts present in the ribonucleic acid from avian influenza virus isolates used in this study, as determined by quantitative real-time reverse transcription polymerase chain reaction.

[H, identifies hemagglutinin gene; N, identifies neuraminidase gene]

Subtype	Isolate	Mean copy count
H4	254	27.932
N7	254	24.355
H5	884	22.982
N2	884	29.947
H5	926	28.264
N2	926	36.872
H5	945	24.908
N2	945	34.225
H5	2216	28.16
N2	2216	37.395
N7	2320	24.11
H2	2355	28.721
N1	2355	26.394
H2	2390	28.883
H1	3455	25.76
N9	3455	24.175
H5	3850	25.349
N2	3850	32.762
H3	13526	30.406
N8	13526	27.095
H6	13618	31.489
N2	13618	29.411
H4	15913	27.092
N6	15913	25.085
H3	16080	26.392
N8	16080	39.83
H2	32425	32.006
N2	32425	29.052
H2	32921	28.306
H3	37536	29.7
N8	37536	26.286
H4	38800	24.417
N6	38800	23.757
H10	40239	28.224
N2	40239	36.346
N9	40459	26.834
H3	44303	30.933
N7	44927	21.845
H10	44939	23.305
N7	44939	21.544
H3	45315	30.857
N6	45315	23.682
H3	45321	28.468
N8	45321	30.8
H1	48944	27.995
N1	48944	26.777
H1	48982	28.418
N1	48982	26.717
H4	49090	28.631
N6	49090	26.112
H1	49176	28.666
N1	49176	26.861
H6	52796	37.785
N2	52796	34.502
H6	56526	33.872
N1	56526	26.071
H4	60390	23.333
N6	60390	22.483
H10	79190	21.526
N9	79190	24.475
H1	100756	28.669
N1	100870	26.675
N9	101124	23.064
N9	103717	22.247
H1	103775	27.775
N1	103775	26.941
H4	103889	23.022
N6	103889	22.115
H3	104839	28.72
N6	104839	23.809
H10	134560	26.822
N7	134560	25.584

of 15 percent CV within the 25–500 bp range. Reactions involving a single HA:NA subtype produced a single amplicon in most of the amplifications. In reactions that did exhibit multiple amplicons, the products were less than 100 bp in size and thus outside the expected range for the desired amplification products.

Results of analysis of amplicon size indicate that the primary product of reactions involving a single HA:NA grouping and targeting a single HA or NA subtype could vary considerably from published values (table 7; Tsukamoto and others, 2012). Target amplicons that varied from published values by more than 10 bp were all smaller than the published values and were mostly HA subtypes, except for N6. Departures from published values tended to increase with increasing amplicon size (data not shown). Calculated standard deviations of amplicon sizes were all low, ranging from 1 to 3.

Corrected molar ratios (eq. 1) obtained for 36 isolates from 13 HA:NA subtypes had a mean ± standard deviation (SD) of 1.63 ± 0.75. Corrected molar ratio calculations produced values (table 8) closer to theoretical perfect value of 1 relative to the simple HA:NA ratio for 22 of the 32 isolates with an improvement toward 1 of 4.50 ± 7.70 (mean ± SD) relative to the simple HA:NA ratio. In the 10 cases where the simple ratio produced values closer to the ideal value of 1, improvement relative to the corrected molar ratio was 0.30 ± 0.36. In HA:NA subtypes for which there were at least four isolates analyzed, corrected molar ratio mean ± standard deviation values were as follows: H1:N1 1.74 ± 0.13, H3:N8 1.41 ± 0.42, H4:N6 1.12 ± 0.07, H5:N2 2.67 ± 1.15.

In mixed samples containing two HA:NA types (fig. 3), the lowest corrected molar ratios (eq. 2) created subtype associations of H3:N8 and H4:N6 (table 9), which accurately reflect the types included in the equation. The H4:N6 combination exhibited the lowest corrected molar ratio (1.09). The H3:N8 combination had a lower ratio (2.03) than the alternative H3:N6 (2.13), indicating that, from an H3 perspective, H3:N8 would be a more viable combination. Pairings are based on the closest fit to the ideal value of 1.00. The combinations of H3:N8 and H4:N6 provide the closest fits for the two HA:NA pairing. Single-size appropriate amplicons were recognized in each of these reactions. The corrected molar ratio for H4:N6 was very close to the mean value for H4:N6 isolates evaluated as a single HA:NA subtype. The actual isolate used in this mix, isolate 49090, (table 8) exhibited a corrected molar ratio 0.05 less when run as a single HA:NA subtype compared to the value obtained when the

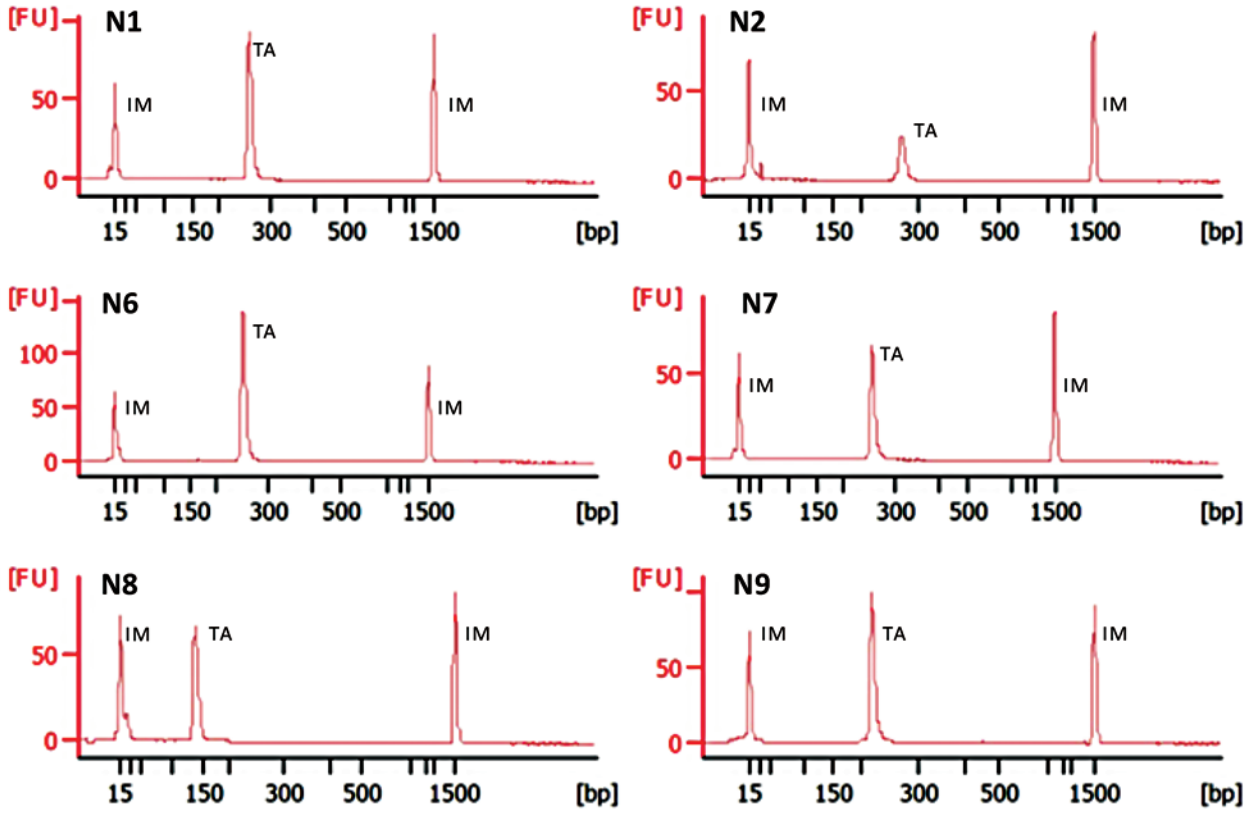

Figure 2. Typical electropherograms of neuraminidase subtypes evaluated in this study as produced by Agilent's Bioanalyzer DNA 1000 and Agilent's 2100 Expert software. Analyses produced from purified and characterized isolates reverse transcribed into deoxyribonucleic acid from purified ribonucleic acid, amplified by reverse transcription quantitative polymerase chain reaction, and then evaluated for amplicon size and molarity. Subtype identification is associated with each graph.

(bp, base pair; FU, fluorescent unit; N, identifies neuraminidase gene; IM, internal marker; TA, subtype-specific target amplicon)

Table 7. Specific amplicon size determined for purified and characterized isolates of avian influenza virus reverse transcribed into complementary deoxyribonucleic acid from purified ribonucleic acid.

[SD, standard deviation; bp, base pair]

Subtype	Number of isolates	Mean ± SD amplicon size (bp)[1]	Departure from published value (bp)[1, 2]
Hemagglutinin			
H2	5	327±2	−16
H4	6	275±1	−10
H6	2	[3]361, 365	−24
Neuraminidase			
N2	8	269±2	−9
N7	5	260±3	−1
N9	4	219±1	−8

[1]Value rounded to nearest whole number. Actual amplicon sizes provided for H6.

[2]From Tsukamoto and others, 2012; based on amplicon mean size.

[3]Mean and standard deviation not determined; 363 used in applicable comparisons.

Table 8. Corrected HA:NA subtype-specific molar ratios determined for amplicons from purified and characterized isolates of avian influenza virus reverse transcribed into cDNA from purified RNA.

[cDNA, complementary deoxyribonucleic acid; RNA, ribonucleic acid; HA or H, hemagglutinin; NA or N, neuraminidase]

HA:NA subtype	Isolate identification[1]	Corrected molar ratio[2]	HA:NA subtype	Isolate identification[1]	Corrected molar ratio[2]
H1:N1	48982	1.81	H4:N6	60390	1.06
H1:N1	100756	1.86	H4:N7	254	1.54
H1:N1	48944	1.75	H5:N2	926	2.02
H1:N9	3455	1.09	H5:N2	2216	4.23
H2:N1	2366	1.17	H5:N2	884	2.38
H3:N6	104839	1.13	H6:N1	56526	1.33
H3:N8	16080	1.21	H10:N1	100870	1.3
H3:N8	45321	2.03	H10:N7	44939	1.26
H4:N6	38800	1.14	H10:N9	79190	1.02

[1]For additional information see table 1.

[2]To facilitate ease of comparison, corrected molar ratios calculated to be between 0.01 and 0.99 were converted to a value greater than one as follows: 1/calculated value.

Table 9. Results from a mixed sample containing two avian influenza virus HA:NA subtypes. Mix produced from purified ribonucleic acid extracted from characterized isolates of avian influenza virus which was reverse transcribed into deoxyribonucleic acid, amplified by quantitative polymerase chain reaction, and then evaluated for amplicon size and molarity.

[bp, base pair; nmol/L, nanomoles per liter; FU, fluorescent unit; HA:NA, hemagglutinin:neuraminidase; H, identifies hemagglutinin gene; N, identifies neuraminidase gene]

Subtype	Predicted fragment size (bp)	Observed fragment size (bp)	Observed molarity (nmol/L)	Amplification strength [FU]	Total molarity (nmol/L)	Potential HA:NA subtype	Corrected molar ratio[1]
H3	358	357	7.5	4.83	7.5	H3:N6	2.13
H4	275	277	26.4	1.92	26.4	H3:N8	2.03
N6	252	258	26.5	2.09	26.5	H4:N6	1.09
N8	137	135	21.4	12.70	27.6	H4:N8	1.23

[1]Calculated as per equation 2.

isolate was part of this mixture. The H3:N8 ratio was outside one single standard deviation for isolates of this HA:NA subtype but was identical to the value obtained from the isolate 45321, which was used in the mixture (table 8).

A second mixed sample containing two HA:NA subtypes was evaluated (fig. 4). In this mix, only three subtypes were present (H4, N6, N7), requiring the use of a different equation for calculating corrected molar ratios (eq. 3). Here, where H4 was the only HA subtype, the corrected molar ratios with N6 and N7 (table 10) were within one standard deviation of the mean from the 31 isolates evaluated individually. The H4 and N7 subtype-specific amplifications produced multiple amplicons with a larger contribution of these additional products to total molarity observed for H4. The H4:N6 corrected ratio was outside one standard deviation of ratios obtained for H4:N6 isolates evaluated in isolation. The corrected ratio for

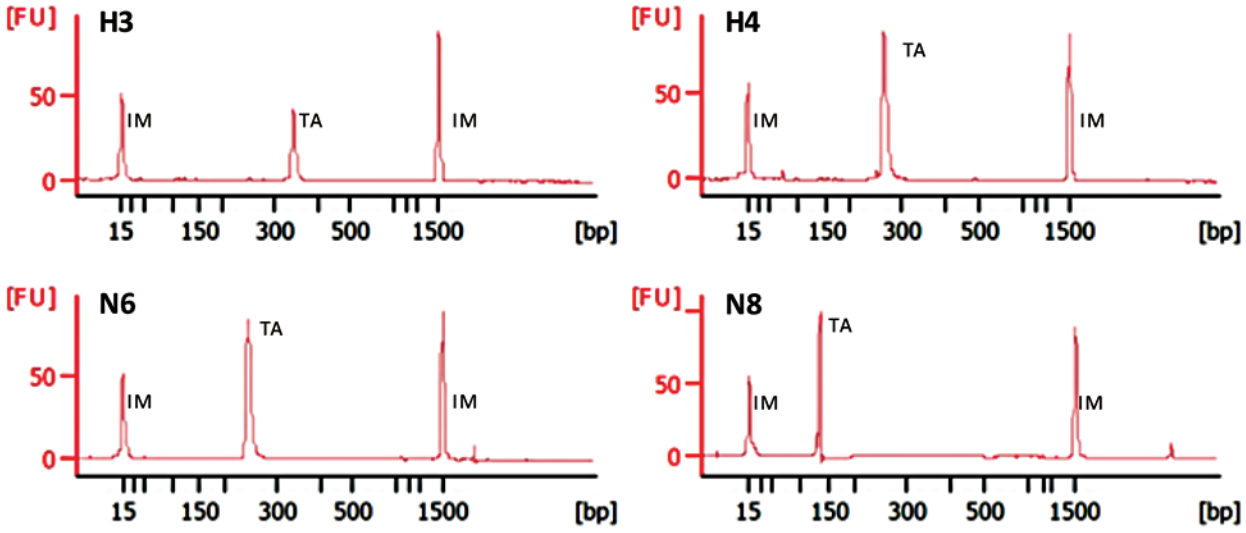

Figure 3. Electropherograms of hemagglutinin and neuraminidase subtypes from a mixed sample containing two avian influenza virus HA:NA subtypes. Analytes produced from purified and characterized isolates reverse transcribed into deoxyribonucleic acid from purified ribonucleic acid, amplified by quantitative polymerase chain reaction, and then evaluated for amplicon size and molarity. Subtype identification is associated with each graph.

(HA:NA, hemagglutinin: neuraminidase; bp, base pair; FU, fluorescent unit; H, identifies hemagglutinin gene; N, identifies neuraminidase gene; IM, internal marker; TA, subtype-specific target amplicon)

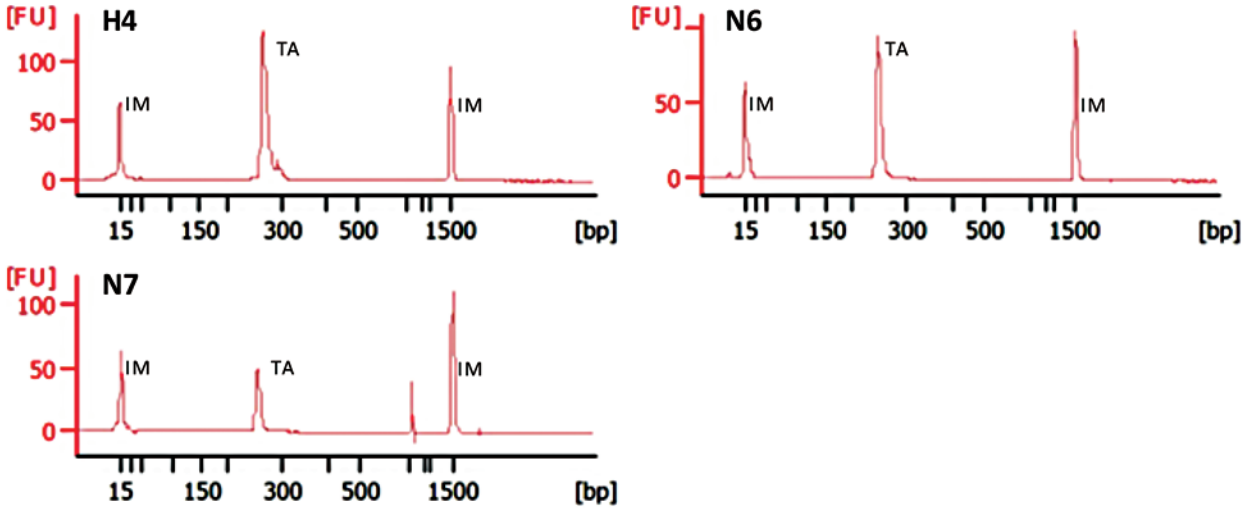

Figure 4. Electropherograms of hemagglutinin and neuraminidase subtypes from a mixed sample containing two avian influenza virus HA:NA subtypes with a shared hemagglutinin subtype. Analytes produced from purified and characterized isolates reverse transcribed into deoxyribonucleic acic from purified ribonucleic acid, amplified by quantitative polymerase chain reaction, and then evaluated for amplicon size and molarity. Subtype identification is associated with each graph.

(HA:NA, hemagglutinin: neuraminidase; FU, fluorescent unit; H, identifies hemagglutinin gene; N, identifies neuraminidase gene; TA, subtype-specific target amplicon; IM, internal marker; bp, base pair)

H4:N7 was slightly lower than the ratio obtained when this HA:NA subtype was evaluated alone (table 8).

To evaluate the efficacy of the method as it relates to environmental samples, we spiked sediment acquired from a pond used by migratory waterfowl using intact virions of the H4:N6 subtype. Our intent here was to simulate actual methods that would be used in environmental surveillance. Analysis of amplified products for H4 and N6 revealed single products in the 100–1,000 bp range (fig. 5). Amplification strengths for H4 and N6 were 1.71 and 2.19, respectively, which are consistent with amplification strength for these subtypes when evaluated directly from allantoic fluid (tables 9 and 10). Molar ratios determined for the spiked H4:N6 were 1.28 (corrected) and 1.14 (not corrected). These values are like those obtained for H4:N6 from allantoic fluid (table 8), indicating that the inclusion of an environmentally relevant substrate had little effect on analysis outcome. The identities of the H4 and N6 subtypes were confirmed by sequencing (tables 3 and 4).

As indicated in process results, the use of RT-qPCR was more effective at establishing ratios closer to the ideal value of 1, as shown by the lower ratio mean ± standard deviation values obtained from the copy count, relative to those produced using corrected molar ratios. Further, the use of amplification efficiency provides a simpler means of ratio correction for AIV RNA obtained from egg cultures.

The relatively high concentrations of RNA from other organisms obtained from direct extraction of environmental samples and the potential variation in the concentration and sequence of this RNA complicates the determination of amplification efficiency by essentially forcing an efficiency determination for each HA and NA subtype in each sample. The use of molar ratios was an attempt to circumvent this issue. Correction of molar ratios from the simple HA:NA equation was necessary because of relative differences in the observed degree of amplification (matrix effect) and because of the production of multiple non-specific products in some reactions. The requirement for determining some measure of amplification efficiency was not eliminated using molarity measures.

Our objective was to evaluate the use of molarity in AIV HA:NA subtype grouping, using robust conditions while still using purified and fully characterized isolates to facilitate methods development. Our final goal was to provide a method application for processes in which RNA extractions are performed directly from samples without intervening viral proliferation steps. The difference in sequence-confirmed target amplicon size relative to those reported by Tsukamoto and others (2012) contributed to the potential variation

Table 10. Results from a mixed sample containing two avian influenza virus HA:NA subtypes sharing a single hemagglutinin subtype. Mix produced from purified ribonucleic acid extracted from characterized isolates of avian influenza virus which was reverse transcribed into deoxyribonucleic acid, amplified by quantitative polymerase chain reaction, and then evaluated for amplicon size and molarity.

[bp, base pair; nmol/L, nanomoles per liter; FU, fluorescent unit; HA:NA, hemagglutinin:neuraminidase; H, identifies hemagglutinin gene; N, identifies neuraminidase gene; --, no additional information intended]

Subtype	Predicted fragment size (bp)	Observed fragment size (bp)	Observed molarity (nmol/L)	Amplification strength [FU]	Total molarity (nmol/L)	Potential HA:NA subtype	Corrected molar ratio[1]
H4	275	267	47.8	2.15	51.5	H4:N6	2.04
N6	252	248	32.9	2.32	32.9	H4:N7	1.21
N7	260	254	14.5	4.04	15.0	--	--

[1]Calculated using equation 3.

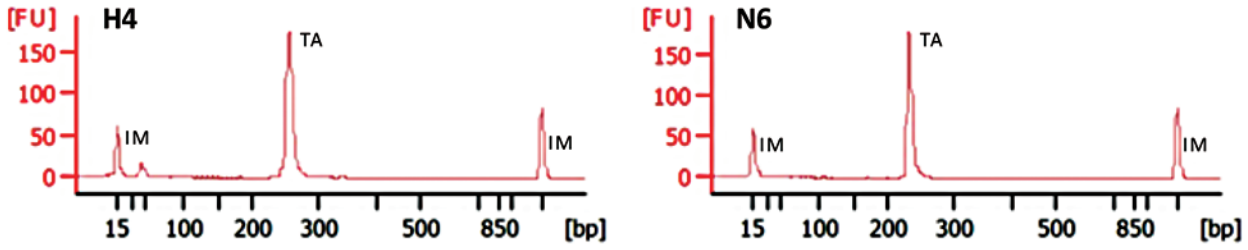

Figure 5. Electropherograms of hemagglutinin and neuraminidase subtypes from pond sediment spiked with intact virus of the H4:N6 avian influenza virus subtype. Analytes produced from reverse transcribed deoxyribonucleic acid from purified virus ribonucleic acid, amplified by quantitative polymerase chain reaction, and then evaluated for amplicon size and molarity. Subtype identification is associated with each graph.

(bp, base pair; FU, fluorescent unit; H, identifies hemagglutinin gene; N, identifies neuraminidase gene; TA, subtype-specific target amplicon; IM, internal marker; bp, base pair)

that was encountered. The isolates used by Tsukamoto and others (2012) were not evaluated, and a different type of qPCR instrument and different reagents were used. The reason for the observed difference in amplicon size was not determined. We can, however, point out that even when all other things are equal, there can be variation in amplicon size within a subtype (table 7) that supersedes known instrument accuracy and reproducibility tolerances. Amplicon size is directly related to molarity and thus to corrected molarity ratios.

Simple HA:NA copy ratios produced from RT-qPCR and molarity can accurately associate AIV HA and NA subtypes into HA:NA groupings. Isolates from some HA:NA subtypes can yield ratios that approach the theoretically perfect value of 1.00, whereas isolates from other HA:NA subtypes consistently produce higher ratios, indicating the presence of HA:NA subtype isolate dependency. Further, the same or very similar ratios can be obtained from isolates whether they are analyzed individually or in an amalgam. The method is not perfect in that we could not account for the increase in corrected molar ratios involving the H4:N6 subtype in mixed samples. Some primer sets used in this study clearly produce amplicons besides those intended, as seen in the electropherograms and in total product molarity. The current equations (eqs. 1–3) take such products into account but do not completely compensate for their effects on the ratio outcome. Despite the imperfections, the method is sufficiently robust to be applicable to complex samples, such as pond sediment. When selecting the RT-qPCR and molarity approaches to group HA and NA subtypes into HA:NA subtypes, we recognized that the same objectives can be accomplished with next generation sequencing technologies, particularly using amplicon resequencing. Such an approach has a distinct advantage in that sequence data are generated directly, thus avoiding the need for follow-up Sanger sequencing to confirm amplicon identity. The results obtained in this study, while promising, are limited in scope and do not completely address the full spectrum of potential issues involved with the association of HA:NA subtypes. Future methods development for the identification of HA:NA subtypes would likely benefit from the inclusion of next-generation sequencing technologies to accelerate the development process and further characterize process requirements.

Acknowledgments

We extend our sincere appreciation to Dr. Andy Ramey of the USGS Alaska Science Center for providing us with the avian influenza virus (AIV)-isolate ribonucleic acid (RNA) used in this study and to Dr. Hon Ip of the USGS National Wildlife Health Center for the isolated virus he provided to Dr. Ramey, making our receipt of the RNA possible. We also thank Dr. Ip for the intact AIV used in our sediment spike experiment.

References Cited

Bowman, A.S., Nolting, J.M., Massengill, R., Baker, J., Workman, J.D., and Slemons, R.D., 2015, Influenza A virus surveillance in waterfowl in Missouri, USA, 2005–2013: Avian Diseases, v. 59, p. 303–308. [Also available at https://doi.org/10.1637/11002-121014-Reg.]

Cheung, T.K.W., and. Poon, L.L.M., 2007, Biology of influenza A virus, *in* Lal, S.K., ed., Biology of emerging viruses: SARS, Avian and human influenza, metapneumovirus, Nipah, West Nile, and Ross River Virus: Annals of the New York Academy Science, v. 1102, p. 1–25.

Lang, A.S., Kelly, A., and Runstadler, J.A., 2008, Prevalence and diversity of avian influenza viruses in environmental reservoirs: Journal of General Virology, v. 89, p. 509–519. [Also available at https://doi.org/10.1099/vir.0.83369-0.]

Machalaba, C.C., Elwood, S.E., Forcella, S., Smith, K.M., Hamilton, K., Jebara, K.B., Swayne, D.E., Webby, R.J., Mumford, E., Mazet, J.A.K., Gaidet, N., Daszak, P., and Karesh, W.B., 2015, Global avian influenza surveillance in wild birds: A strategy to capture viral Diversity: Emerging Infectious Diseases, v. 21, p. e1–e7, accessed January 25, 2018, at https://wwwnc.cdc.gov/eid/article/21/4/14-1415_article.

Payungporn, S., Chutinimitkul, S., Chaisingh, A., Damrongwantanapokin, S., Buranathai, C., Amonsin, A., Theamboonlers, A., and Poovorawan, Y., 2006, Single step mutilplex real-time RT-PCR for H5N1 influenza A virus detection: Journal of Virological Methods, v. 131, p. 143–147. [Also available at https://doi.org/10.1016/j.jviromet.2005.08.004.]

Pearce, J.M., Ramey, A.M., Flint, P.L., Koehler, A.V., Fleskes, J.P., Franson, J.C., Hall J.S., Derksen, D.V., and Ip, H.S., 2009, Avian influenza at both ends of a migratory flyway: Characterizing viral genomic diversity to optimize surveillance plans for North America: Evolutionary Applications, v. 2, p. 457–468. [Also available at https://doi.org/10.1111/j.1752-4571.2009.00071.x.]

Pearce, J.M., Ramey, A.M., Ip, H.S., and Gill R.E., 2010, Limited evidence of trans-hemispheric movement of avian influenza viruses among contemporary North American shorebird isolates: Virus Research, v. 148, p. 44–50. [Also available https://doi.org/10.1016/j.virusres.2009.12.002.]

Pearce, J.M., Reeves, A.B., Ramey, A.M., Hupp, J.W., Ip, H.S., Bertram, M., Petrula, M.J., Scotton, B.D., Trust, B., Meixell, K.A., and Runstadler, J.A., 2011 Interspecific exchange of avian influenza virus genes in Alaska: The influence of trans-hemispheric migratory tendency and breeding ground sympatry: Molecular Ecology, v. 20, p. 1015–1025. [Also available at https://doi.org/10.1111/j.1365-294X.2010.04908.x.]

Ramey, A.M., Pearce, J.M., Ely, C.R., Sheffield Guy, L.M., Irons, D.B., Derksen, D.V., and Ip, H.S., 2010a, Transmission and reassortment of avian influenza viruses at the Asian—North American interface: Virology, v. 406, p. 352–359. [Also available at https://doi.org/10.1016/j.virol.2010.07.031.]

Ramey, A.M., Pearce, J.M., Flint, P.L., Ip, H.S., Derksen, D.V., Franson, J.C., Petrula, M.J., Scotton, B.D., Sowl, K.M., Wege, M.L., and Trust, K.A., 2010b, Intercontinental reassortment and genomic variation of low pathogenic avian influenza viruses isolated from Northern Pintails (*Anas acuta*) in Alaska: Examining the evidence through space and time: Virology, v. 401, p.179–189.

Ramey, A.M., Pearce, J.M., Reeves, A.B., Franson, J.C., Petersen, M.R., and Ip, H.S., 2011, Evidence for limited exchange of avian influenza viruses between seaducks and dabbling ducks at Alaska Peninsula coastal lagoons: Archives of Virology, v. 156, p. 1813–1821. [Also available at https://doi.org/10.1007/s00705-011-1059-z.]

Reeves, A.B., Pearce, J.M., Ramey, A.M., Ely, C.R., Schmutz, J.A., Flint, P.L., Derksen, D.V., Ip, H.S., and Trust, K.A., 2013, Genomic analysis of avian influenza virus from waterfowl in western Alaska, USA: Journal of Wildlife Disease, v. 49, p. 600–610. [Also available at https://doi.org/10.7589/2012-04-108.]

Stech O., Veits, J., Abdelwhab, E.S.M., Wessels, U., Mettenleiter, T.C., and Stech, J., 2015, The neuraminidase stalk deletion serves as major virulence determinant of H5N1 influenza viruses in chicken: Scientific Reports, v. 5., Article number 13493, accessed January 25, 2018, at https://www.nature.com/articles/srep13493.

Tsukamoto K., Javier, C.P., Shishido, M., Noguchi, D., Pearce, J., Kang, H.-M., Jeong, O.M., Lee, Y-J., Nakanishi, K., and Ashizawa, T., 2012, SYBR Green-based real-time reverse transcription-PCR for typing and subtyping of all hemagglutinin and neuraminidase genes of avian influenza viruses and comparison to standard serological subtyping tests: Journal of Clinical Microbiology, v. 50, p. 37–45. [Also available at https://doi.org/10.1128/JCM.01195-11.]

Wittwer, C.T., Herrmann, M.G., Moss, A.A., and Rasmussen, R.P., 1997, Continuous fluorescence monitoring of rapid cycle DNA amplification: Biotechniques, v. 22, p. 130–138.

For additional information, contact:
Director, Leetown Science Center
U.S. Geological Survey
11649 Leetown Road
Kearneysville, WV 25430

or visit our website at:
https://www.lsc.usgs.gov

Publishing support provided by West Trenton Publishing Service Center

ISSN 2331–1258 (online)
https://doi.org/10.3133/ofr20181102